NASA TECHNICAL MEMORANDUM

NASA TM X-2833

NASA TM X-2833

DYNAMIC RESPONSE OF MACH 2.5 AXISYMMETRIC INLET WITH 40 PERCENT SUPERSONIC INTERNAL AREA CONTRACTION

by Robert J. Baumbick, Robert E. Wallhagen, George H. Neiner, and Peter G. Batterton

Lewis Research Center
Cleveland, Ohio 44135

NATIONAL AERONAUTICS AND SPACE ADMINISTRATION • WASHINGTON, D. C. • JULY 1973

1. Report No.	2. Government Accession No.	3. Recipient's Catalog No.
NASA TM X-2833		
4. Title and Subtitle DYNAMIC RESPONSE OF MACH 2.5 AXISYMMETRIC INLET WITH 40 PERCENT SUPERSONIC INTERNAL AREA CONTRACTION		5. Report Date July 1973
		6. Performing Organization Code
7. Author(s) Robert J. Baumbick, Robert E. Wallhagen, George H. Neiner, and Peter G. Batterton		8. Performing Organization Report No. E-7426
9. Performing Organization Name and Address Lewis Research Center National Aeronautics and Space Administration Cleveland, Ohio 44135		10. Work Unit No. 501-24
		11. Contract or Grant No.
12. Sponsoring Agency Name and Address National Aeronautics and Space Administration Washington, D.C. 20546		13. Type of Report and Period Covered Technical Memorandum
		14. Sponsoring Agency Code
15. Supplementary Notes		

16. Abstract

Results of experimental tests conducted on a supersonic, mixed-compression, axisymmetric inlet are presented. The inlet is designed for operation at Mach 2.5 with a turbofan engine (TF-30). The inlet was terminated with either a choked-orifice plate or a long pipe with variable area choked exit plug. Frequency responses were obtained for selected static pressures in the diffuser. These pressures were selected as potential control signals for terminal shock control. Frequency responses were obtained for the Mach 2 and 2.5 conditions for different terminations. Responses also were obtained with and without cowl bleed. Internal disturbances were produced by sinusoidally varying the inlet overboard bypass doors at frequencies out to 100 hertz.

17. Key Words (Suggested by Author(s))	18. Distribution Statement
Supersonic inlets Air intake Supersonic inlet dynamics Mixed compression inlets	Unclassified - unlimited

19. Security Classif. (of this report)	20. Security Classif. (of this page)	21. No. of Pages	22. Price*
Unclassified	Unclassified	19	$3.00

* For sale by the National Technical Information Service, Springfield, Virginia 22151

DYNAMIC RESPONSE OF MACH 2.5 AXISYMMETRIC INLET WITH 40 PERCENT SUPERSONIC INTERNAL AREA CONTRACTION

by Robert J. Baumbick, Robert E. Wallhagen, George H. Neiner, and Peter G. Batterton

Lewis Research Center

SUMMARY

Results of experimental tests conducted on a supersonic, mixed-compression, axisymmetric inlet are presented. The inlet is designed for operation at Mach 2.5 with a turbofan engine (TF-30). The inlet was terminated with either a choked-orifice plate or a long pipe with variable area choked exit plug.

Frequency responses were obtained for selected static pressures in the diffuser. These pressures were selected as potential control signals for terminal shock control. Frequency responses were obtained for the Mach 2 and 2.5 conditions for different terminations. Responses also were obtained with and without cowl bleed. Internal disturbances were produced by sinusoidally varying the inlet overboard bypass doors at frequencies out to 100 hertz.

In general, coupling the inlet to the long pipe produced multiple resonances in the static-pressure frequency response. The response of static pressures with the inlet coupled to the choked-orifice plate shows resonance occurring beyond 100 hertz.

INTRODUCTION

The function of the supersonic inlet is to convert the kinetic energy of the supersonic stream to static pressure rise at the engine compressor face with minimum losses and low distortion. In a mixed-compression inlet maximum pressure recovery and low distortion levels are achieved with the normal shock located just downstream of the inlet's throat. Inlet controls are needed to prevent normal shock displacement from this critical point when internal or external disturbances are introduced. Controls development requires some knowledge of the open-loop dynamic characteristics of the inlet. The open-loop dynamics serve to identify the critical frequencies of the inlet.

This program is an extension of past programs on inlet dynamics conducted at the Lewis Research Center. Reference 1 presents dynamic test results on a small scale, Mach 2.5 axisymmetric inlet. Reference 2 presents results of dynamic tests conducted on a Mach 2.7, two-dimensional inlet. An example of a dynamic test program conducted in industry is given in reference 3. An inlet dynamics program was conducted in the Lewis 10- by 10-Foot Supersonic Wind Tunnel with an axisymmetric, mixed-compression inlet designed for Mach 2.5 operation with a TF-30 engine. This dynamics program was run to identify the inlet dynamic characteristic. With this information a terminal shock control will be developed to be used in inlet-engine tests. The inlet was subjected to symmetrical and unsymmetrical disturbances, produced by varying the overboard bypass area at frequencies up to 100 hertz. Data were obtained at Mach 2 and 2.5 with and without cowl bleed and with either a choked orifice, located at the compressor face station, or the long pipe, terminated in a choked flow plug, coupled to the inlet. The effect of an engine termination on the inlet dynamic characteristic is expected to be similar to either the choked orifice or long pipe or some combination of the two.

Analytical expressions for inlet dynamics are presented. These were obtained by curve fitting experimental frequency response data to transfer functions. The experimental results are presented in Bode form. The amplitude results are normalized to the 0.1-hertz value.

SYMBOLS

A bypass-door area, cm^2

P static inlet pressure, N/cm^2

$\bar{P}$ average static inlet pressure, N/cm^2

s Laplace operator, 1/sec

X_s used in figures to identify steady-state shock operating point, distance from cowl lip, cm

Subscripts:

23 represents transducer located 23.77 cm from cowl lip

56 represents transducer located 56.79 cm from cowl lip

66 represents transducer located 66.95 cm from cowl lip

APPARATUS AND PROCEDURE

Model

The inlet (fig. 1) is an axisymmetric, mixed-compression inlet with translating centerbody and with 40 percent internal supersonic area contraction. The inlet is designed for Mach 2.5 operation with a TF-30 engine. Operation of the inlet at Mach 2 is achieved by changing centerbody cones. The inlet has a capture area of 7070 square centimeters and measures 180 centimeters from cowl lip to compressor face. Provisions are made for boundary-layer bleed on the centerbody and cowl. Porous bleeds are located on the cowl and flow is ducted overboard. The centerbody bleed is a slot type bleed. The centerbody bleed flow is ducted to four equally spaced struts located in the diffuser section. Centerbody bleed flow is controlled by a butterfly valve in each strut. The butterfly valves are actuated by electric motors. The inlet was tested with a cowl bleed configuration determined in a steady-state program (unpublished data) and also with all cowl bleeds sealed.

The inlet is equipped with eight overboard bypass doors used to match inlet-engine airflow. Figure 2 shows a cross section of the diffuser indicating the location of the bypass doors and the centerbody flow struts.

All the tests were run at zero angle of attack. The inlet was alternately coupled to a choked orifice, located at the compressor face station, or to a long pipe (487 cm), which was terminated in a remotely controlled choked plug.

Dynamic data were obtained for terminal shock operating points located from 2.54 to 8.87 centimeters from the inlet's throat. Inlet and tunnel conditions for this program are listed in table I.

Disturbance Device

Internal airflow disturbances are produced with the inlet overboard bypass doors. Installation of a door on the inlet is shown in figure 1. The bypass door is a sliding plate valve driven by a high-response electrohydraulic servovalve-actuator assembly. Each door has a wide open area of 404 square centimeters for a linear motion of 2.54 centimeters. Detailed information on the bypass doors used in this test program is presented in reference 4. Reference 5 contains detailed information on the design of electrohydraulic servosystems.

Sufficient shock displacements were achieved using one door with a zero-to-peak amplitude of 6 percent of full stroke linear motion. For this reason only one or two doors were used at any one time. With two doors the zero-to-peak disturbance amplitude was 3 percent of full stroke. The frequency response of door motion to a sinusoidal input signal is flat (no reduction in zero-to-peak amplitude from steady state) to approximately 100 hertz for both the 3 and 6 percent stroke cases.

Instrumentation

Linear motion of the bypass door is measured by a linear variable differential transformer (LVDT). The transducer has negligible dynamics in the frequency range covered in these tests (0.1 to 100 Hz).

Figure 3 is a sketch of the inlet showing the pressure instrumentation locations. Steady-state pressure instrumentation were used to measure the terminal shock position. These 16 steady-state transducers start at a distance of 23 centimeters from the cowl lip, and extend to a point 66 centimeters from the cowl lip. The 14 transducers further upstream are spaced 2.54 centimeters apart. The last two are spaced 5.08 centimeters apart.

The dynamic pressures were measured with strain gage type transducers connected to the cowl with short tubes. The frequency response of the pressure measuring system had negligible dynamics in the range covered in these tests (0.1 to 100 Hz). As shown in figure 3, the planes containing the dynamic instrumentation are located at 56 and 66 centimeters from the cowl lip. Each plane contains four transducers, spaced 90° apart, which were electrically averaged. The average pressures are identified as $\overline{P}_{56}$ and $\overline{P}_{66}$. Responses are also presented for single pressures, identified as P_{56} and P_{66}, located at 35° (see fig. 3). The location of the geometric throat and the cowl bleed downstream of the throat are shown in figure 3.

Data Acquisition and Reduction

Dynamic data were reduced on line using a commercial discrete frequency-response analyzer. Dynamic data were also taken on analog tape using sweep-frequency techniques. The data were then reduced off line on a digital computer using methods described in reference 6. The data are presented as Bode plots (amplitude ratio and phase difference against frequency). The data presented are for both single pressures P_{56} and P_{66} (at 35°, fig. 3) and average pressures $\overline{P}_{56}$ and $\overline{P}_{66}$ in response to bypass-door area variations. The amplitude data are normalized to the 0.1-hertz value.

RESULTS AND DISCUSSION

Open-Loop Dynamics

The pressures P_{56} and P_{66} are considered as potential feedback signals for closed-loop shock control. Since there is no dynamic shock sensor on this inlet, pressures P_{56} and P_{66} are used to infer shock position. Steady-state gains were obtained by setting up a given shock excursion and taking the ratio of the change in pressures P_{56} and P_{66} and the corresponding bypass area change. The terminal shock operating point was not consistent for all the runs. Each figure therefore contains information on the shock operating point for each case. The symbol X_s in the figures represents the distance of the shock operating point in centimeters from the cowl lip.

Effects of Unsymmetrical Airflow Disturbances

Frequency response plots of pressures P_{56} and P_{66} for unsymmetrical airflow disturbances are shown in figures 4 and 5, respectively. These data were obtained for Mach 2 operating conditions with the nominal bleed configuration and long-pipe termination. The unsymmetrical disturbances were applied by using doors 1 and 5 separately. The operating points for figures 4 and 5 are indicated in the figures. The results show more phase lag when door 5 is used for the disturbance, which is expected because door 5 is farther away from the pressure measuring station. The amplitude ratios show a dependence on disturbance location. Figure 4 indicates the normalized amplitude ratio of P_{56} is attenuated more when door 1 is used for disturbance, however, the steady-state gain is higher for door 1. This may result from the fact that P_{56} is closer to the shock and is more strongly affected by shock skewing due to the unsymmetrical disturbance. Coupling the inlet to the long pipe results in resonances at approximately 30 to 60 hertz. A slight shift in the resonant frequency is detected for the different disturbance location. The amplitude ratio of P_{56} is down 30 percent at approximately 1.5 hertz. The amplitude ratio of P_{66} is down 30 percent at approximately 3.5 hertz.

Effect of Inlet Terminations

The results shown in figures 6 and 7 are a comparison of the choked-orifice and long-pipe terminations. Results shown in figure 6 are for Mach 2 conditions with the nominal bleed configuration. In figure 7 the results shown are for Mach 2.5 operating conditions with the nominal bleed configuration. The orifice was designed for a TF-30 engine match point at Mach 2.5 conditions and was not properly sized for Mach 2 operation. The amplitude responses, shown in figure 6 shows a corner frequency at 3.5 hertz. The term corner frequency, as used here, is taken to mean the frequency at which the normalized frequency response is reduced 30 percent from the steady-state value. The long-pipe termination would be expected to result in a lower corner frequency because of the large additional volume of the long pipe. However, the reduction in volume seems to be cancelled by the larger resistance of the orifice, which resulted from improper sizing, and results in approximately the same corner frequency for both terminations. In figure 7 the amplitude ratio of P_{66} has a corner frequency of 3 hertz for the long-pipe termination and 10 hertz for the choked-orifice plate. Here the effect of the large volume is apparent. The steady-state terminal shock was located at different points for the data shown in figures 6 and 7, and this may be the cause of some of the difference in response in each figure. Observations based on the results shown in figures 6 and 7 indicate that the long pipe introduces resonances at approximately 30 and 60 hertz and that the choked-orifice plate shows resonance occurring beyond 100 hertz. The shift to higher resonant frequency for the choked orifice is expected because the effective inlet length is shorter.

Effect of Cowl Bleed Configurations

Results presented in figure 8 are for Mach 2.5 operating conditions with the choked-orifice termination with and without cowl bleed. In figure 9 the results shown are for Mach 2.5 operating conditions with the long-pipe termination with and without cowl bleeds. The results shown in these figures indicate that the normalized amplitude ratio show more attenuation when the cowl bleeds are sealed. But the steady-state gains are larger with sealed bleeds, and the unnormalized response would show that more attenuated amplitude ratios result with cowl bleeds. With cowl bleeds sealed shock position and therefore diffuser static pressures are more sensitive to downstream disturbances.

Effect of Signal Averaging

Responses of the electrically averaged signals obtained with the sweep-frequency techniques are shown in figures 10 and 11. In figure 10 the results are shown for $\overline{P}_{56}$ and $\overline{P}_{66}$ for Mach 2.5 conditions with cowl bleeds sealed with choked-orifice termination. In figure 11 the results are shown for $\overline{P}_{56}$ and $\overline{P}_{66}$ for Mach 2.5 conditions with nominal cowl bleed with long-pipe termination. Average pressure $\overline{P}_{56}$ shows more phase lag than $\overline{P}_{66}$ since $\overline{P}_{56}$ is further away from the point of disturbance. No difference in the response occurred when either door pairs 1 and 5 or 3 and 7 were used.

No differences were found between the responses of P_{56} and $\bar{P}_{56}$ or between P_{66} and $\bar{P}_{66}$. Using average pressures results in some reduction of noise normally inherent in a single pressure measurement and averages out the effect of shock skewing.

Transfer Function Representation

Results shown in figures 12 and 13 represent the transfer functions obtained by curve fitting the experimental data. In each figure both the experimental data and the transfer function results are shown together. The transfer function shown in figure 12 indicates that, for a choked-orifice termination, a first-order lag occurs at 33 radians per second (5.2 hertz) and second-order effects show a natural frequency at 508 radians per second with damping ratio of 0.336. The transfer function obtained for long-pipe termination (see fig. 13 for $\bar{P}_{66}$) is much more complex because of the multiple resonances occurring in the experimental data.

SUMMARY OF RESULTS

Results presented show the effect of unsymmetrical disturbances on the response of diffuser cowl static pressures P_{56} and P_{66}. Both pressures show a marked dependence on disturbance location beyond approximately 55 hertz. Pressure P_{56}, being closer to the downstream excursion of the shock is more sensitive to disturbance location because of shock skewing caused by the unsymmetrical disturbance.

Coupling the inlet to a long pipe produces resonances at approximately 30 and 60 hertz. With the choked-orifice termination the first resonance is moved to beyond 100 hertz.

The results for Mach 2 indicate a corner frequency of 3.5 hertz for both terminations because the choked orifice is improperly sized for this condition. The increased resistance, due to the improperly sized orifice, seems to cancel the reduced volume effect when the choked-orifice termination is used.

For Mach 2.5 conditions the inlet coupled to an orifice show a corner frequency of approximately 10 hertz. With the long-pipe termination the corner frequency is reduced to 3 hertz illustrating the effect of the additional volume. For the Mach 2.5 case the exit areas were the same for both terminations.

Results show that the terminal shock and consequently diffuser static pressures are more sensitive to downstream disturbances when cowl bleeds are sealed.

Analytical expressions were obtained from experimental data with a curve fit program. These expressions are in the transfer function form and closely represent the response of the static pressures for both terminations considered.

Lewis Research Center,
National Aeronautics and Space Administration,
Cleveland, Ohio, May 8, 1973,
501-24

REFERENCES

1. Wasserbauer, Joseph F.: Dynamic Response of a Mach 2.5 Axisymmetric Inlet With Engine or Cold Pipe and Utilizing 60 Percent Supersonic Internal Area Contraction. NASA TN D-5338, 1969.
2. Baumbick, Robert J.; Neiner, George H.; and Cole, Gary L.: Experimental Dynamic Response of a Two-Dimensional, Mach 2.7, Mixed-Compression Inlet. NASA TN D-6957, 1972.
3. Chun, K. S.; and Burr, R. H.: A Control System Concept and Substantiation Test For An Axisymmetric Mixed Compression Supersonic Inlet. Paper 68-581, AIAA, June 1968.
4. Webb, John A., Jr.; Mehmed, Oral; and Hiller, Kirby W.: Improved Design of a High-Response Slotted-Plate Overboard Bypass Valve for Supersonic Inlets. NASA TM X-2812, 1973.
5. Zeller, John R.; and Webb, John A., Jr.: Determination and Evaluation of Performance Limit Criteria of Fast-Response Electrohydraulic Servosystems. NASA TM X-2736, 1973.
6. Milner, Edward J.; and Bruton, William M.: Application of a Hybrid Computer to Sweep Frequency Data Processing. NASA TM X-2753, 1973.

TABLE I. - INLET AND TUNNEL TEST CONDITIONS

Tunnel free-stream conditions				Inlet conditions	
Mach number	Total pressure, N/cm^2	Total temperature, K	Reynolds number per meter, Re/m	Choked exit corrected airflow, kg/sec	Termination
2	6.90	310	8.188×10^6	81.0	Long pipe
2	6.89	309	8.188×10^6	66.6	Choke plate
2.5	8.77	308	8.188×10^6	66.6	Choke plate
2.5	8.74	317	8.188×10^6	64.3	Long pipe

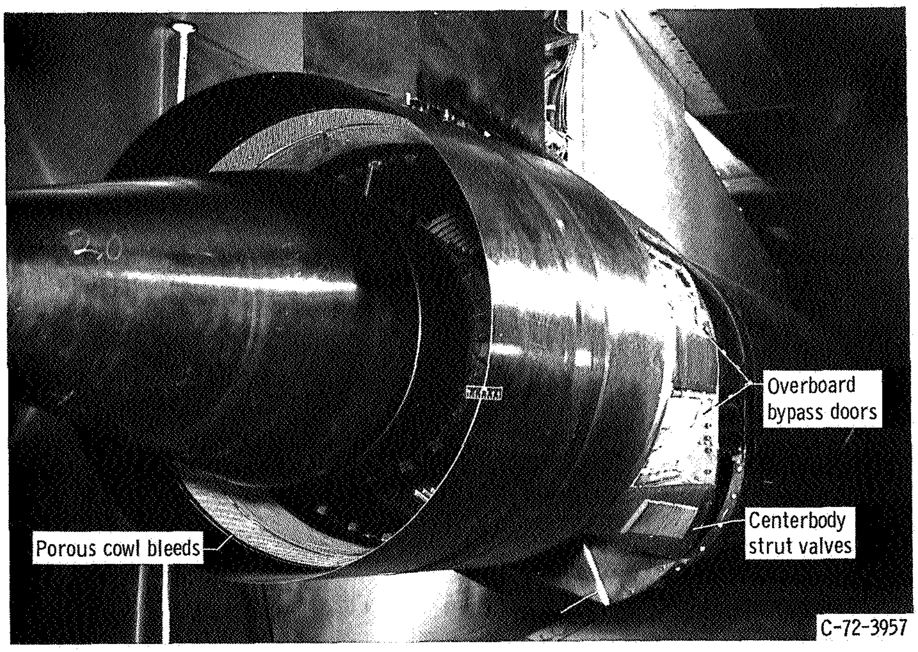

Figure 1. - Inlet installed in test section.

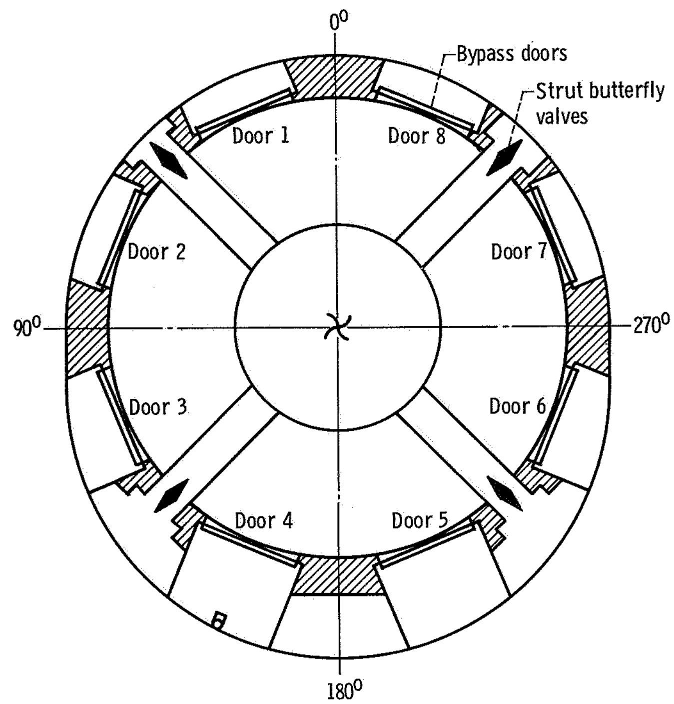

Figure 2. - View of inlet looking downstream showing bypass door and centerbody bleed flow struts.

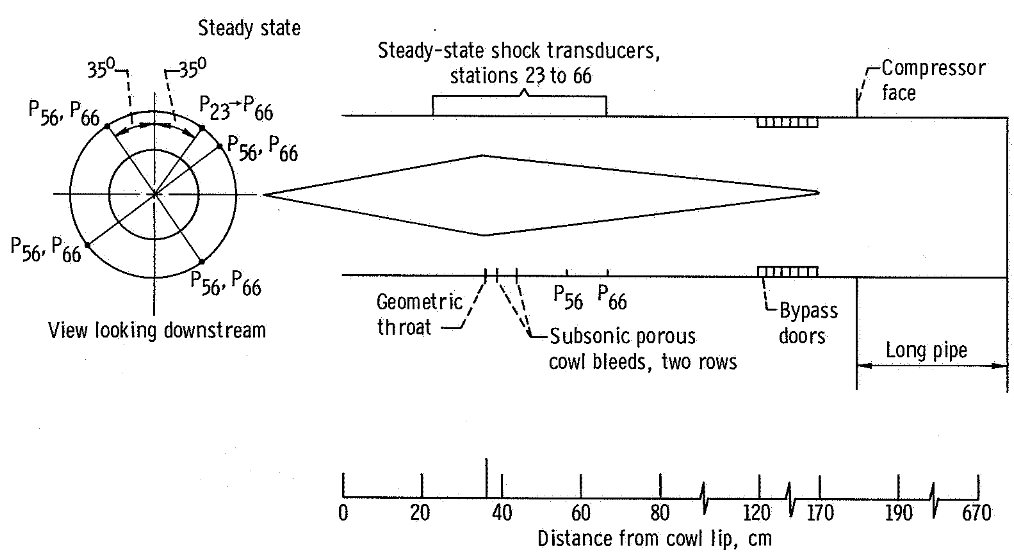

Figure 3. - Location of steady state and dynamic instrumentation on inlet.

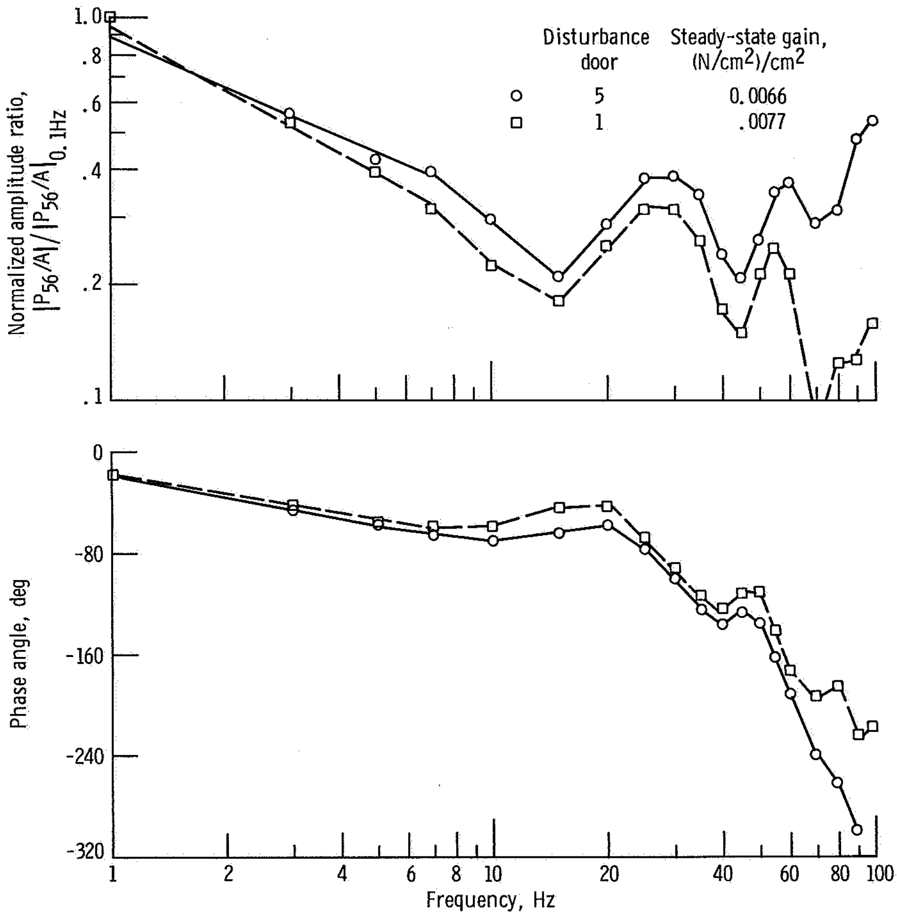

Figure 4. - Frequency response of P_{56} showing effect of unsymmetrical disturbances. Mach 2 conditions with cowl bleed and long-pipe termination; shock operating point, 45.4 centimeters from cowl lip.

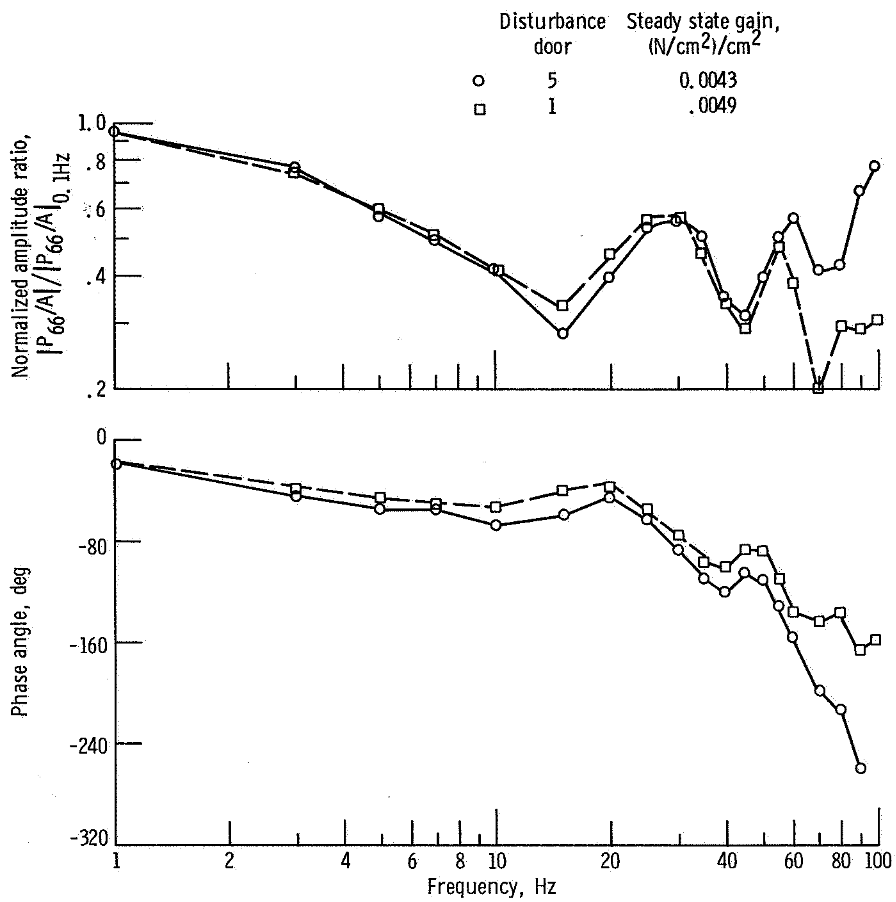

Figure 5. - Frequency response of P_{66} showing effect of unsymmetrical disturbances. Mach 2 conditions with cowl bleed and long-pipe termination; shock operating point, 45.4 centimeters from cowl lip.

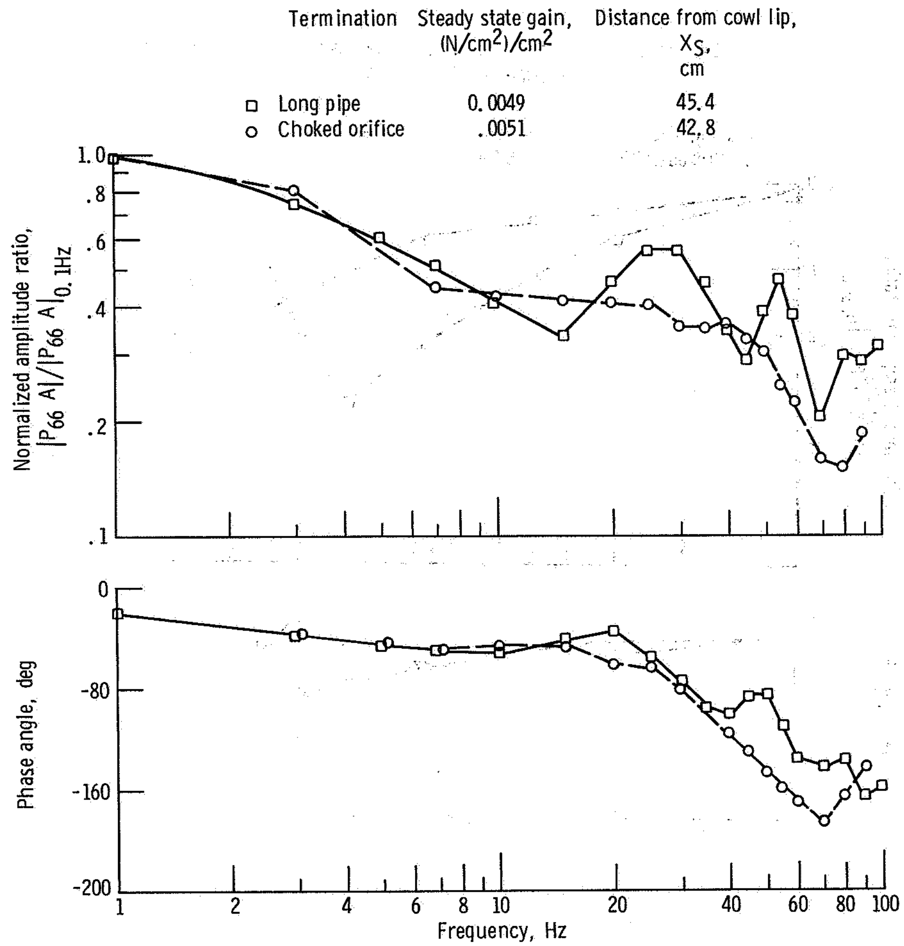

Figure 6. - Frequency response of P_{66}, for Mach 2 conditions, with cowl bleed and door 1 used for disturbance, and for different terminations.

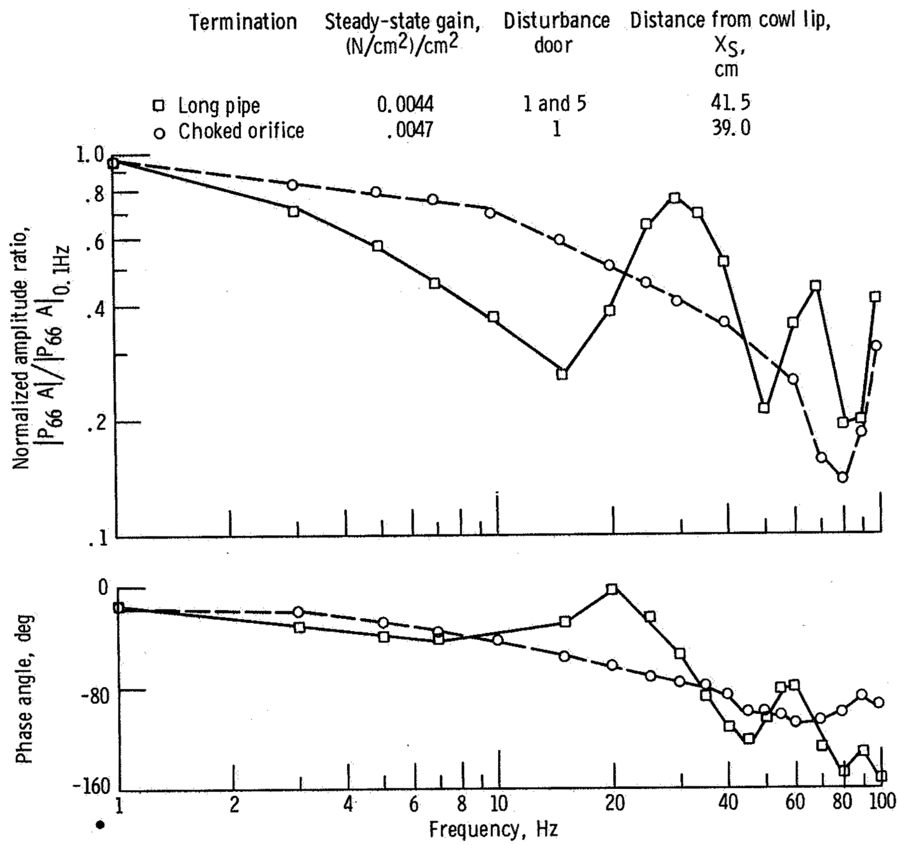

Figure 7. - Frequency response of P_{66}, for Mach 2.5 conditions, with cowl bleed, and for different terminations.

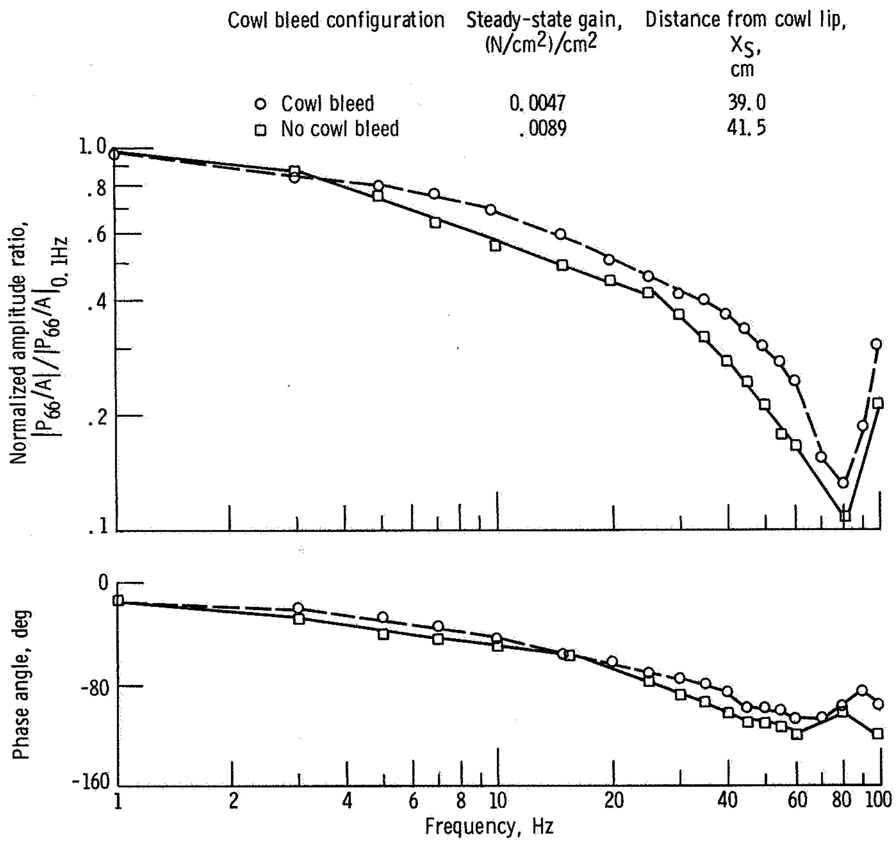

Figure 8. - Frequency response of P_{66} for Mach 2.5 conditions, with door 1 used for disturbance and with choked-orifice termination, and for different bleed configurations.

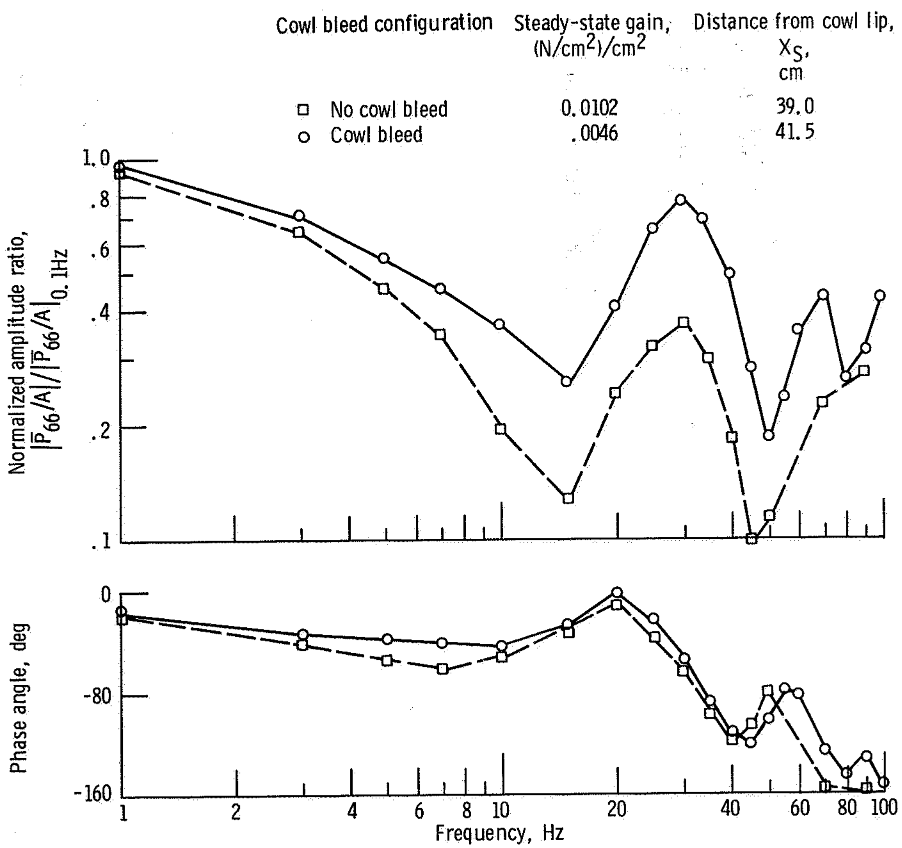

Figure 9. - Frequency response of $\bar{P}_{66}$ for Mach 2.5 conditions, with doors 1 and 5 used for disturbance and long-pipe termination, and for different bleed configurations.

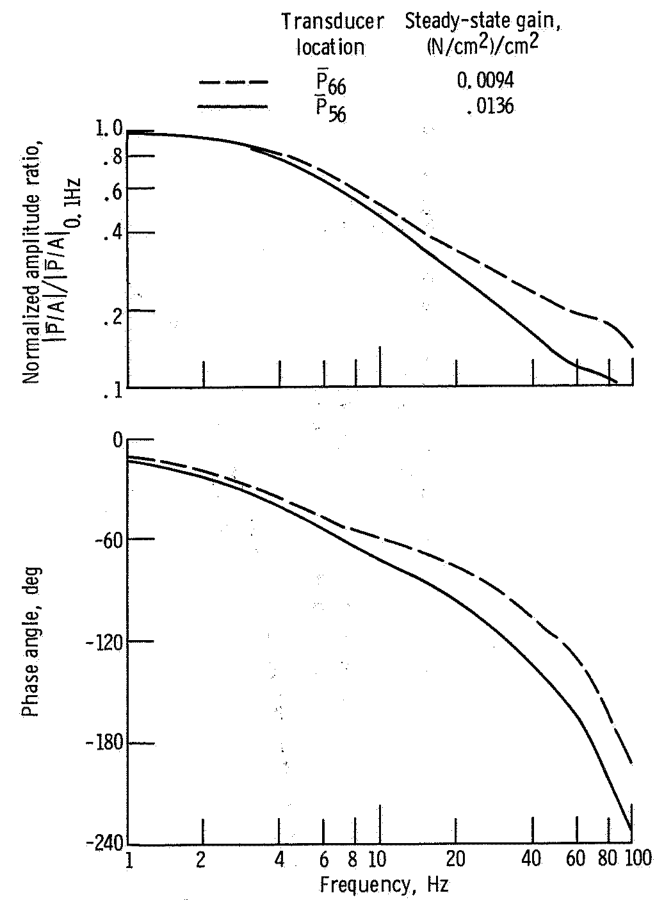

Figure 10. - Frequency response of diffuser static pressures for Mach 2.5 conditions with doors 3 and 7 used for disturbance. No cowl bleed; choked-orifice termination; shock location, 41.5 centimeters from cowl lip.

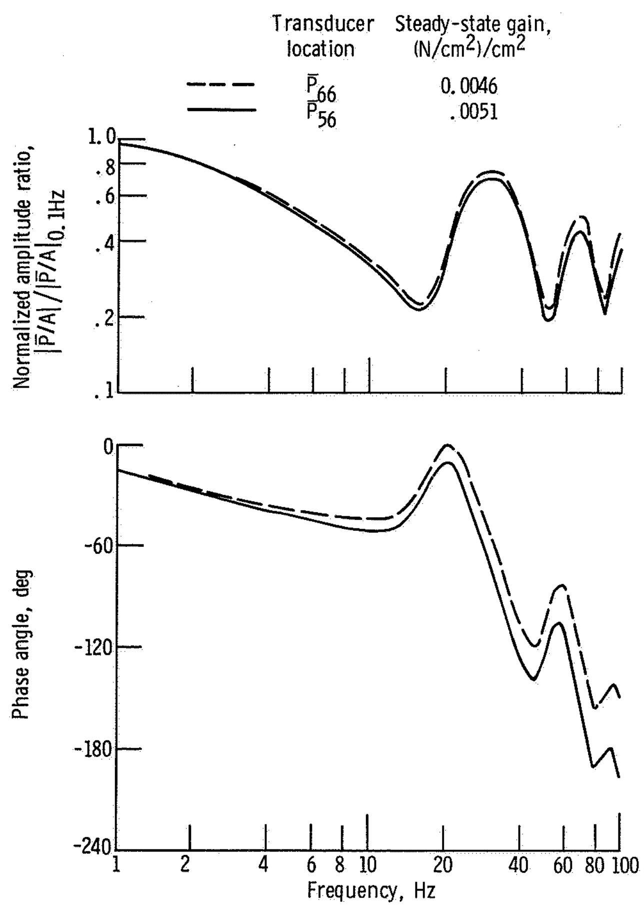

Figure 11. - Frequency response of diffuser static pressures for Mach 2.5 conditions with doors 3 and 7 used for disturbance. Nominal cowl bleed; long-pipe termination; shock location, 41.5 centimeters from cowl lip.

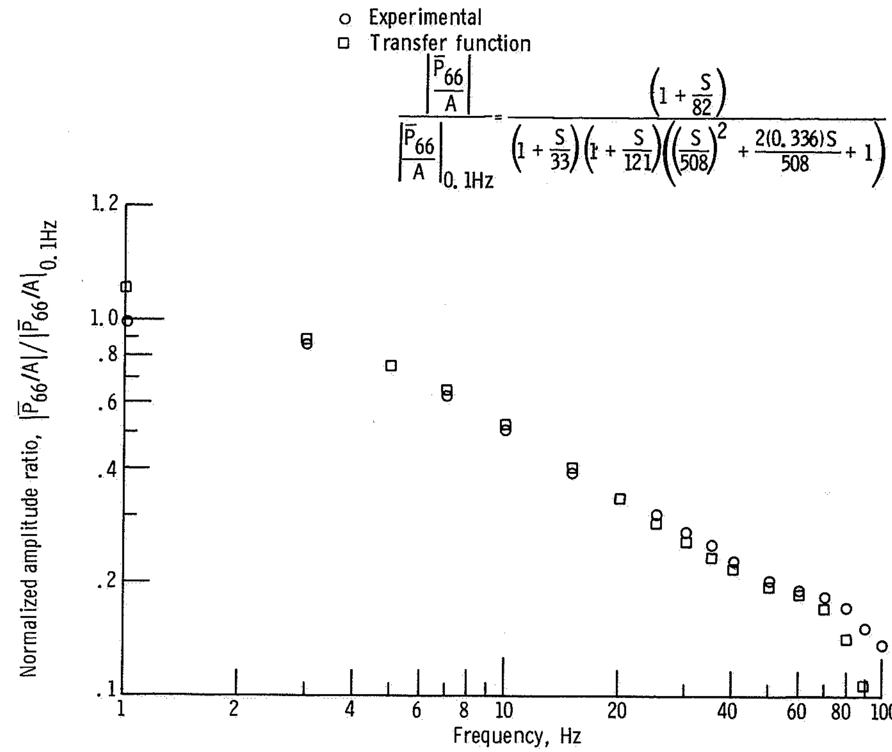

Figure 12. - Amplitude ratio comparison of synthesized transfer function with experimental data for Mach 2.5 conditions, no cowl bleed, and choked-orifice termination.

$$\frac{\left|\frac{\bar{P}_{66}}{A}\right|}{\left|\frac{\bar{P}_{66}}{A}\right|_{0.1\mathrm{Hz}}} = \frac{\left[\left(\frac{S}{94}\right)^2 + \frac{2(0.46)S}{94} + 1\right]\left[\left(\frac{S}{322}\right)^2 + \frac{2(0.07)S}{322} + 1\right]\left[\left(\frac{S}{14112}\right)^2 + \frac{2(0.57)S}{14112} + 1\right]}{\left[1 + \frac{S}{24}\right]\left[\left(\frac{S}{183}\right)^2 + \frac{2(0.25)S}{183} + 1\right]\left[\left(\frac{S}{362}\right)^2 + \frac{2(0.16)S}{362} + 1\right]\left[\left(\frac{S}{540}\right)^2 + \frac{2(0.5)S}{540} + 1\right]}$$

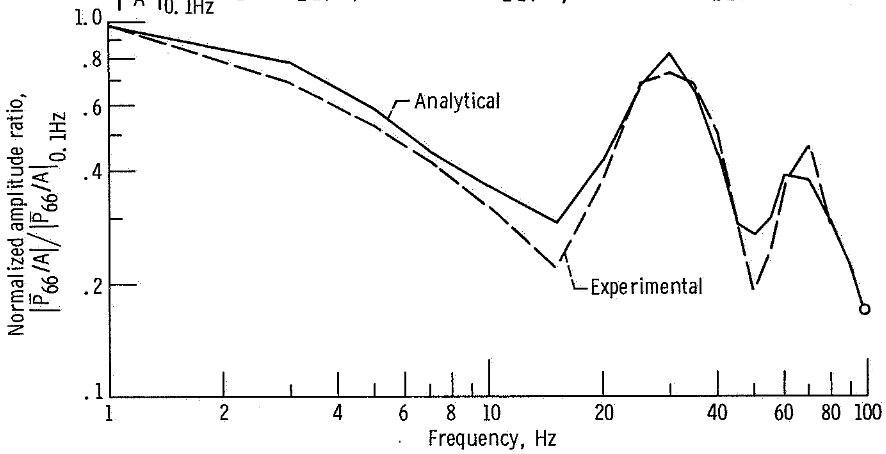

Figure 13. - Amplitude ratio comparison of synthesized transfer function with experimental data for Mach 2.5 conditions, nominal cowl bleed, and long-pipe termination.

NASA-Langley, 1973 —— 28 E-7426